Lasers in Manufacturing Conference 2015

Fundamental analysis of hot cracks in remote laser welded aluminium fillet welds

Hans Langrieger[a,b,*], Frank Krafft[c], Martin Mensinger[d], Florian Oefele[a]

[a]BMW AG, Petuelring 130, München 80809, Germany
[b]TUM Graduate School, Boltzmannstraße 17, Garching 85748, Germany
[c]Hochschule München, Lothstraße 34, München 80335, Germany
[d]Lehrstuhl für Metallbau, Arcisstraße 21, München 80333, Germany

Abstract

Remote laser welding is a highly efficient technology for the automotive body in white series production. However, the application of remote laser welding to high strength aluminium alloys is restricted due to hot cracking. Recent research activities mainly focus on centerline hot cracks in welds in close-edge position. Crack-free welds can be created within an edge distance of smaller than 2 mm. In this study remote laser welded fillet joints of high strength EN AW-6082 T6 alloy were analyzed experimentally concerning their hot cracking behavior. This type of joint design can avoid centerline cracks. Yet, cracks in transverse direction on a microscopic scale were found along the weld seam by x-ray radiography. Scanning electron microscope images confirmed that the cracks formed in semi-solid-state. In order to investigate the influence of welding parameters on the formation of transverse hot cracks a full factorial study regarding the welding speed, the laser power, the sheet thickness, the protrusion of the lower sheet and the beam position was conducted. In this study the welding speed and laser power were found to have a major effect on hot crack formation. Additionally high-speed imaging was used to observe the exact moment and the location of hot crack formation. It can be seen that transverse hot cracks arise not at the end of the weld pool but beside the weld pool between the weld centerline and the seam edge. As the solidification behavior during the welding process is a key factor in hot crack formation the influence of melt pool geometry on hot crack formation was investigated by high-speed imaging. Based on these results a beam oscillation method was developed to control the melt pool morphology leading to reduced hot cracks in fillet joints.

Keywords: remote laser welding; fillet welds; transverse hot cracks; high strength aluminium

* Corresponding author. Tel.: +4989-382-15635
E-mail address: hans.langrieger@bmw.de

1. Introduction

1.1. Motivation

Lightweight construction is a key technology in automotive design to achieve fuel efficiency targets and fulfill customer expectations regarding the handling characteristics of new cars. In order to reduce the weight of the vehicles high strength aluminium alloys are used increasingly in body in white construction [Heidrich, 2010].

One challenging aspect concerning the use of aluminium alloys in a series production is the joining technology. High availability with low cycle times and high quality is required as well as low production costs. At the moment cold joining technologies like riveting or clueing and warm joining technologies like arc welding or laser welding are being used predominantly.

Remote laser welding offers the possibility to increase productivity. Remote means, that the laser beam is focused at a distance of about 500 – 800 mm of the work piece [Zaeh et al., 2010]. By this way cycle times can be reduced further. As high strength aluminium alloys are susceptible to hot cracks, the application of remote laser welding has been restricted to non-hot crack sensitive materials so far. Therefore further research activities are necessary to enlarge the use of remote laser welding to high strength aluminium alloys.

1.2. State of the art

The formation of hot cracks is associated with the presence of low melting phases between already solidified dendrites and a load on that liquid film resulting from solidification shrinkage [Schuster, 2004]. A summary of different hot cracking mechanisms was made by *Katgerman and Eskin* [Katgerman and Eskin, 2008].

In aluminium alloys the hot crack susceptibility depends on the content of silicon and magnesium. Unfortunately 6xxx aluminium alloys, which are often used in the automotive sector, are very crack-sensitive [Dilthey, 2005]. To avoid hot cracking filler materials or multi-layer fusion alloys are used to change the chemical composition of the weld seam [Schinzel, 2002; Coniglio et al., 2008; Weller et al., 2013].

In his studies Rapp points out that the occurrence of hot cracks is related to the melt pool morphology. A low welding speed leads to a high curved melt pool resulting in fine grains and therefore only in few or even no hot cracks, as the fine weld structure better withstands the shrinkage load. On the other hand a high welding speed leads to a teardrop shaped melt pool. Therefore big columnar dendrites grow leading to numerous hot cracks [Rapp, 1996]. *Tang* also focuses on the correlation between weld grain size and hot crack formation. The hot crack susceptibility could be reduced by adding grain-refining elements like Ti/B [Tang, 2014].

Recent research focuses on centerline hot cracks in close-edge position. Crack free welds can be created in a distance of lower than 2 mm or more than 5 mm to the free edge [Hilbinger, 2000; Ploshikhin et al., 2005; Stritt et al., 2012].

Following this idea the objective of this paper is a fundamental analysis of the hot crack behavior of remote laser welded fillet welds. This paper wants to answer the question of how different welding setups and welding parameters influence hot cracking. A special focus lays on the relation of melt pool geometry and the formation of transverse hot cracks. Fillet weld joint design couldn´t have been established so far because of the problem of accurate beam position on the edge of the sheets. However, nowadays camera based tracking systems are available that allow a high precise beam position for remote welding systems [Oefele and Roos, 2014].

2. Methods

2.1. Experimental setup

All experiments were conducted with a 6 kW IPG fiber laser YLS-6000 emitting a wavelength of 1068 – 1080 nm. The beam was delivered to the focusing optic by an optical fiber with a core diameter of 100 µm. The laser beam was focused by a SCANLAB intelliWELD 30 FC V scanner optic with a focal length of 660 mm and an image scale of 1:6 leading to a 600 µm focus diameter on the surface of the work piece. Prior to welding experiments a caustic measurement was performed with Primes FocusMonitor to verify the beam characteristics. Aluminium alloy EN AW-6082-T6 with a thickness of 1.2 and 2.5 mm was used. Table 1 shows the chemical composition of the used material measured by an optical emission spectrometer.

Table 1. Chemical composition of EN AW-6082-T6

EN AW-6082	Unit	Si	Fe	Cu	Mn	Mg	Cr	Zn	Ti	Others
nominal	(%)	0.7 – 1.3	max 0.50	max 0.10	0.4 – 1.0	0.6 – 1.2	max 0.25	max 0.25	max 0.10	max 0.15
1.2 mm	(%)	0.87	0.4	0.06	0.59	0.88	0.02	0.01	0.02	0.01
2.5 mm	(%)	0.86	0.28	0.001	0.62	0.78	0.002	0.008	0.02	0.01

All experiments were carried out without use of shielding gas except some trials where it is specifically stated. In this case Argon with a flow rate of 30 l/min was delivered to the welding zone by a pipe with a diameter of 8 mm. The sheets were fixed with a clamping device using a pneumatic tensioning cylinder as shown in Fig. 1. Stoppers at the clamping device ensured the repeatability of the sheet position. Additionally the front end of the upper sheet that faces the stoppers was milled to ensure a planar contact.

To examine the melt pool geometry during the ongoing welding process a high-speed camera iSpeed 3 by Olympus working at a frame rate of 5000/s was used. The experimental setup is shown in Fig. 1.
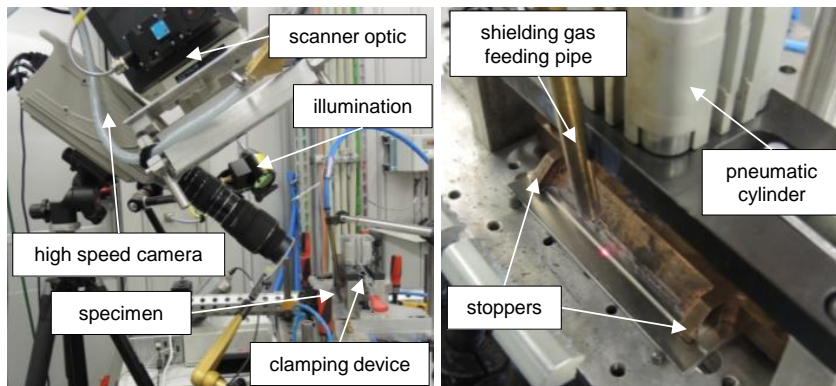

Fig. 1. Experimental setup

The camera was positioned at a fixed place perpendicular to the welding direction. The lateral angle of the camera was 52° based normal to the surface of the welded sheets. Image distortion was considered in all image analyses and all measured data were corrected by a trigonometrical function.

To study the hot crack behavior of aluminium fillet welds a full factorial experimental design was chosen. The used parameters are listed in Table 2. The preselection of the examined parameters was done by specialist knowledge considering the state of the art. The parameter setting was determined by pretests in the run up to the study.

Table 2. Experimental design

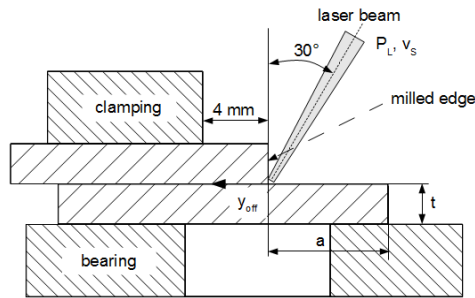| Parameter	Laser power	Welding speed	Beam offset	Protrusion of lower sheet	Thickness of lower sheet
Unit	P_L (kW)	v_s (m/min)	y_{off} (mm)	a (mm)	t (mm)
Value	3.2 / 3.95 / 4.7	5 / 7 / 9	0 / 0.4 / 0.8	4 / 7.4 / 10.8	1.2 / 2.5

Fig. 2. Welding setup

Fig. 2 shows a schematic drawing of the welding setup. The beam started 20 mm indented sideways from the sheet edge and was guided on a straight line along the work piece. The seam length was 70 mm.

2.2. Experimental analysis

To evaluate the hot cracking behavior every weld seam was tested by a General Electric x-ray installation phoenix micromex DXR-HD with a resolution of detail of up to 0.5 µm. As an indicator for the hot cracking susceptibility of different welding setups the number of cracks was counted and divided by the seam length.
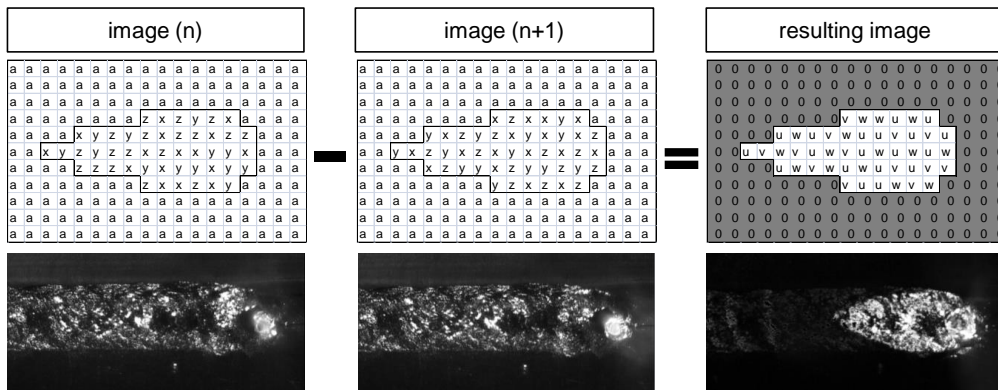

Fig. 3. Procedure of image processing

The measurement of the weld pool geometry was done by high-speed images. The melt pool border was made visible with image processing utilizing the movement of liquid metall. The schematic procedure is illustrated in Fig. 3.

The high-speed images were saved as arrays. Every pixel of an image has an entry in the array with the associated grey scale color code. The entries in the array of two sequent pictures changes only in the area of the melt pool because of light reflection on the moving surface of the liquid metal. If the arrays are deducted the area of the melt pool gets bright and the area of solidified material gets dark. By this procedure an image with clearly highlighted melt pool borders can be created as seen in Fig. 3.

3. Results and Discussion

Different types of cracks were observed during the remote laser welding of aluminium fillets. On the one hand centerline cracks on a macroscopic scale were found after welding (Fig. 4b). Centerline cracks always appeared in full-penetrated welds and a protrusion of the lower sheet of less than 7.4 mm. No centerline cracks were observed in partial penetrated welds regardless of the protrusion of the lower sheet or in samples with more than 7.4 mm protrusion as seen in Fig. 4a). This is in good agreement with analysis reported for overlap welds or bead on plate welds. [Bachhofer, 2000; Waldmann, 2001; Hilbinger, 2000].
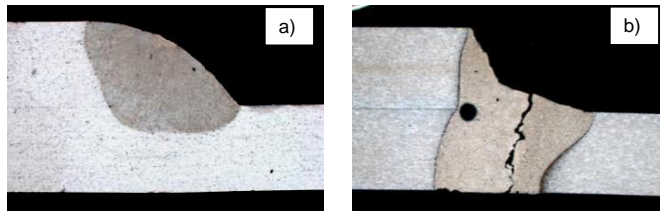

Fig. 4. Cross-section polish a) P_L = 3.2 kW; v_S = 5 m/min; y_{off} = 0.8 mm; a = 4 mm; t = 1.2 mm; b) P_L = 3.2 kW; v_S = 7 m/min; y_{off} = 0 mm; a = 4 mm; t = 1.2 mm

However, transverse cracks on a microscopic scale were found by x-ray radiography as illustrated in Fig. 5. Microscopic means that the crack is only visible with a magnification of more than 6-fold [DIN EN ISO 6520-1]. The propagation of these transverse cracks was limited to the molten areas. The quantity and the size of the cracks strongly depended on the welding parameters. Some cracks spread over the entire weld and some cracks only covered the edge of the weld seam edge.
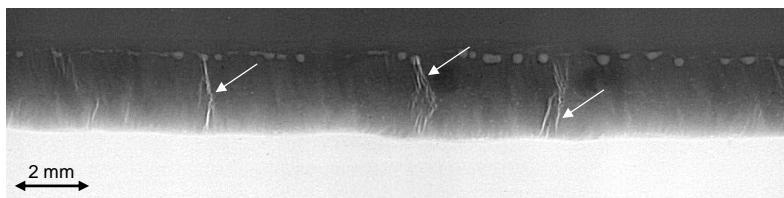

2 mm

Fig. 5. X-ray image 120 kV/90 µA; P_L = 4.7 kW; v_S = 7 m/min; y_{off} = 0.8 mm; a = 7.4 mm; t = 1.2 mm

Scanning electron microscope (SEM) images of the fracture interfaces showed a smooth surface. This confirmed that the cracks formed in semi solid state during solidification. Fig. 6 shows images of the SEM. The two images on the upper right side (2) are made in the center of the weld seam. The image on the upper left side (1) is made on the edge of the weld seam. By comparing both images the different phases of crack

formation can be seen. Whereas the image on the left side shows a very smooth surface and no sign of liquid rupture the picture on the right side shows a separation just before solidification.
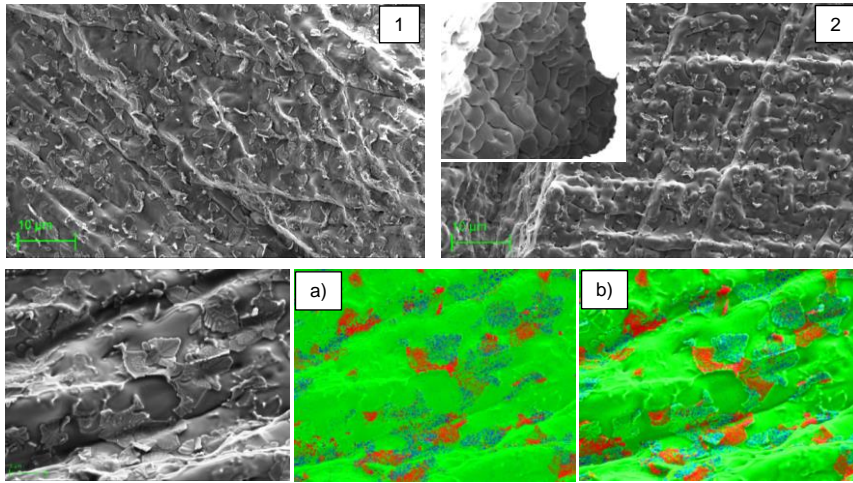

Fig. 6. Scanning electron microscope image of crack surface and EDX mapping; a) green:Al, blue:Fe, red:Si; b) green:Al, blue:Fe, red:Mg

By higher magnification of SEM images micro segregations can be seen on the surface. Energy dispersive X-ray analysis identified the segregations to be Al_xFe_x and Mg_xSi_x phases (Fig. 6). Al_xFe_x phases were reported before to be responsible for building low melting eutectics [Hilbinger, 2000].

In order to get a better understanding of the mechanism of transverse hot crack formation the welding process was observed with a high speed camera.
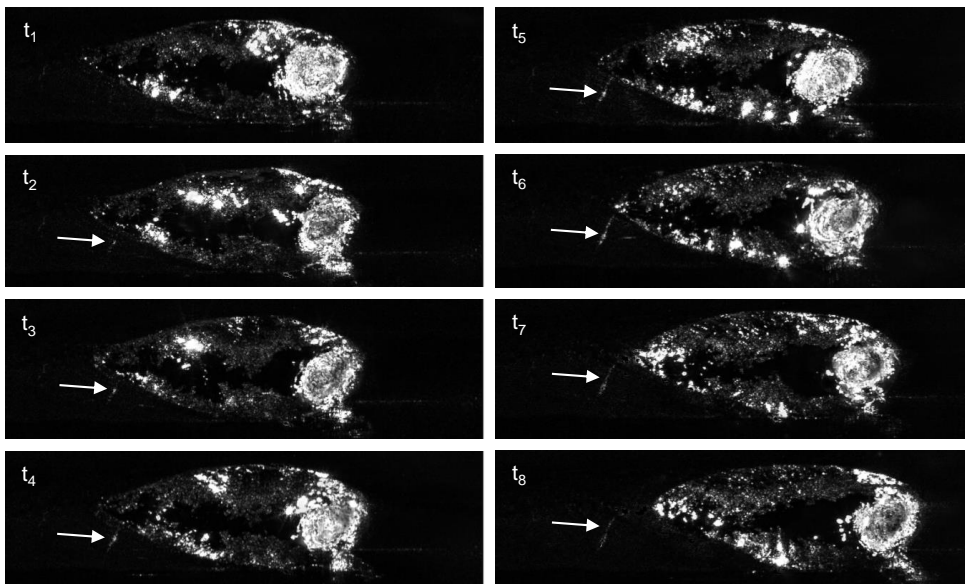

Fig. 7. Transverse crack formation and growth

As the surface of the weld seam is pretty rough without shielding gas, Argon is used to ensure a smooth surface and hence make the formation of cracks visible. Fig. 7 illustrates a welding sequence of 10 ms while the welding process is in steady state.

The first picture of the sequence is marked with t_1 the last picture of the sequence is marked with t_8. It can be seen that the crack forms at the rear area beside of the melt pool and propagates subsequently to the middle and the edge of the weld seam. This behavior is contrary to *Pellini's* theory who assumed that transverse hot cracks arise in the heat affected zone and afterwards spread into the molten area [Pellini, 1952]. At the time of t_5 the newly formed crack is connected with the melt pool but no feeding with liquid metal – so-called heeling – occurs.

A major subject of this study is to identify how the hot crack susceptibility is influenced by different welding parameters. Based on the experimental design listed in table 2 and evaluation of 127 weld seams by X-ray radiography a multiple regression model of the hot crack susceptibility was created which is illustrated in Fig. 7. Due to restrictions in the experimental design concerning the deep penetration welding threshold the laser power was increased in parameter sets with 3.2 kW and high welding speed until keyhole welding was possible. The hot crack susceptibility was measured by the number of transverse hot cracks per mm weld seam. End crater cracks and samples with a centerline line crack were not included in the model.
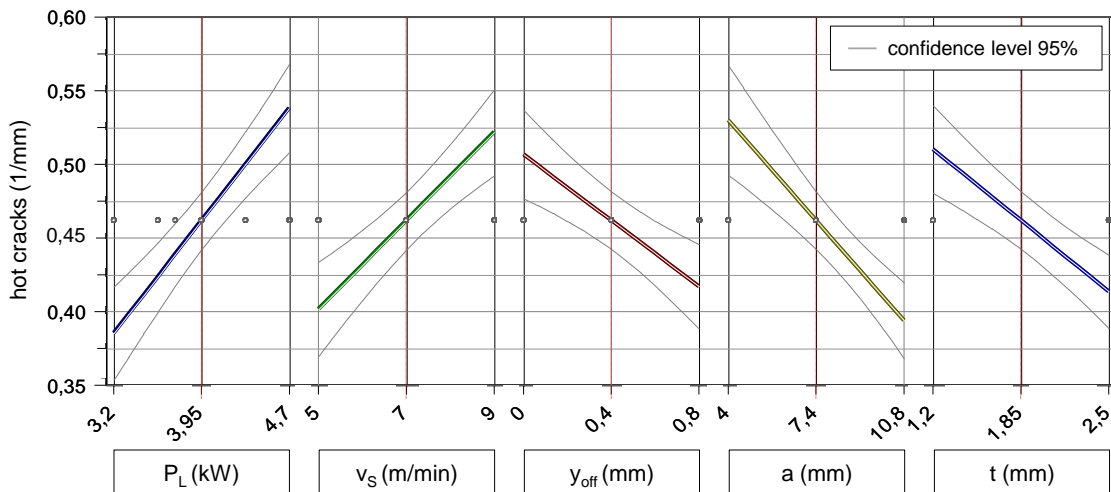

Fig. 8. Influence of welding parameters on the hot crack susceptibility (multiple regression)

It can be seen that the hot crack susceptibility increases with growing laser power and welding speed which is in good agreement with previous studies [Rapp, 1996; Ehrhardt, 1999; Hu and Richardson, 2006]. Although the laser power and welding speed are presented as two independent parameters in this model, it is favorable to look at them as linked parameters as proposed by *Ploshikhin et al.* [Ploshikhin et al., 2004]. As the laser power and welding speed are responsible for the energy input into the work piece and certain energy is needed to achieve the prescribed welding depth it is not possible to increase the welding speed without adjusting the laser power.

The hot crack susceptibility decreases with increasing beam position to the upper sheet, increasing protrusion of the lower sheet and increasing sheet thickness of the lower sheet.

According to *Rapp* the melt pool geometry has a strong influence on the hot crack formation. As mentioned in the state of the art chapter the melt pool geometry is mainly determined by the welding speed. Therefore the angle between the seam edge and the melt pool border – in this paper called γ - as an

indicator of the melt pool geometry was measured by high speed-imaging. Fig. 9 illustrates two examples of high speed-images at different welding speeds. The laser power was adjusted to reach a similar welding depth. It can be seen that the length and shape of the meld pool changes with welding speed. During solidification the dendrites grow perpendicular to the solid/liquid border and along the highest thermal gradient [David and Vitek, 1989]. Therefore an elongated melt pool supports the growth of columnar dendrites and the hot cracking susceptibility increases (Fig. 9b).
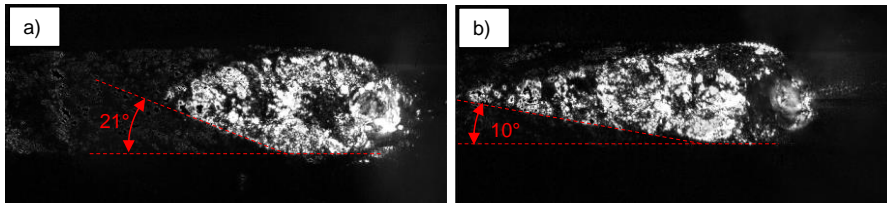

Fig. 9. Melt pool geometry a) P_L = 3.1 kW; v_s = 5 m/min; y_{off} = 0.0 mm; a = 10.8 mm; t = 2.5 mm; b) P_L = 4.4 kW; v_s = 9 m/min; y_{off} = 0.0 mm; a = 10.8 mm; t = 2.5 mm

In fillet welds the shape of the melt pool is not only determined by the welding speed but also by the beam offset respective to the upper sheet, in this paper called y_{off}. As can be seen in Fig. 10 (left) γ decreases with increasing welding speed but there is a strong influence of the beam offset, too. The angle γ increases by a growing beam offset. That is a possible explanation why the hot cracking susceptibility decreases with increasing beam offset as shown in Fig. 8.
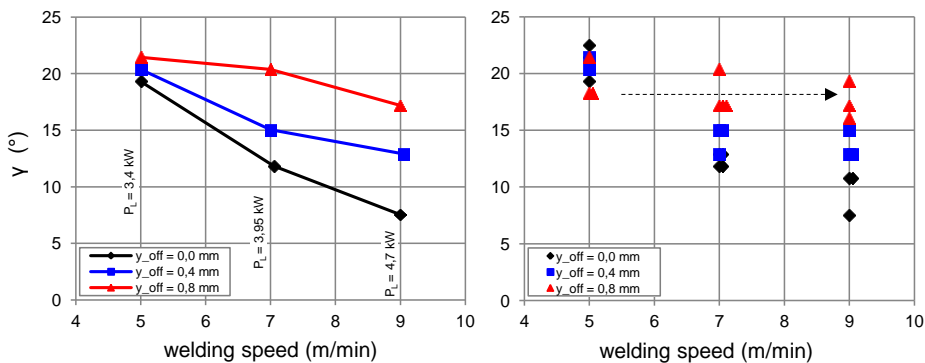

Fig. 10. Melt pool geometry against welding speed and beam offset[1]

This picture slightly changes if the laser power is considered additionally. In the left graph of Fig. 9 the laser power is kept constant for a certain welding speed. On the contrary the measured data on the right graph were created by varying the laser power in a range of 200 – 600 W. In case of 0.8 mm beam offset there are some examples in which γ doesn't decrease with increasing welding speed but stays on the same level or even increases. Nevertheless, the number of hot cracks still increased with rising welding speed. This indicates that there has to be an additional reason for hot crack formation beside the melt pool geometry.

---

[1]γ is corrected by the image distortion caused by the tilt position of the high speed camera

Hu and Richardson attributed transverse cracking in laser/arc hybrid welding of 7xxx Al-alloys to an elongated temperature distribution which causes a rising tensile stress in the fusion zone [Hu and Richardson, 2006]. Hence, the formation of hot cracks has always to be considered as an interaction between metallurgical and thermo mechanical factors. How these interactions exactly look like is still an unknown field as only few studies exists which consider both factors.

Two different fundamental approaches exist to prevent hot cracking. One possibility is to control the load on the mush zone during welding with an additional heat source [Ploshikhin et al., 2005]. Beside this, there is a metallurgical approach that tends to control either the chemical composition of the weld or to optimise the solidification process. For example *Zhang et al.* proposed temporal pulse shaping to prevent hot cracking during Nd:YAG welding of EN AW-6061 T6 aluminium alloy [Zhang et al., 2008]. However, the disadvantage of pulsed laser welding is a low average output power and therefore a limited field of application.

In this study beam oscillation was used to reduce hot cracking. The aim of beam oscillation is the generation of an elliptical melt pool with a high curvature at the end and thereby a globular weld grain structure. This is achieved by a low frequent circular ($A_x = A_y$) movement of the laser spot. Additionally a low welding speed was chosen, to minimize the shrinkage load. As can be seen in Fig. 11 the melt pool shape is more elliptical caused by the spatial distributed energy deposition. Thus, X-ray radiography showed no hot cracks in the weld seam.
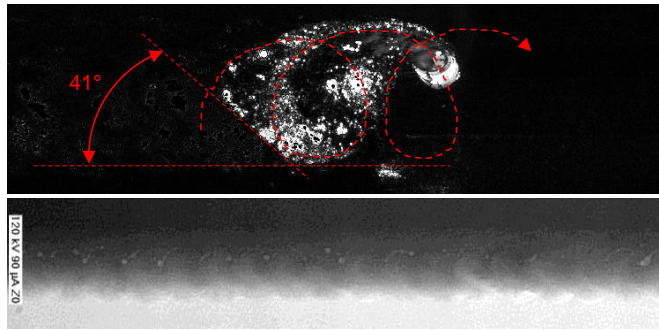

Fig. 11. Control of melt pool geometry by beam oscillation P_L = 3.2 kW; v_S = 5 m/min; y_{off} = 0.7 mm; a = 10.8 mm; t = 2.5 mm; f = 75 Hz; $A_x = A_y$ = 0.7 mm

The advantage of this method is that no additional hardware or software is necessary, as low frequent beam oscillation is feasible with standard remote scanner optics. Furthermore it is still possible to weld in a keyhole process and therefore no restrictions in sheet thickness exist.

4. Conclusion and Future Work

In this paper a fundamental analysis of the hot cracking behaviour of remote laser welded high strength aluminium fillet welds is presented. The results can be summarized in three points:

1.) Centerline line hot cracks can be avoided by fillet weld joint design in remote laser welding of high strength aluminium alloy. Transverse hot cracks on a microscopic scale arise along the weld seam.
2.) High-speed images during welding indicate that the melt pool geometry alone cannot explain a rising number of transverse hot cracks with increasing welding speed in fillet welds.
3.) By means of low frequent circular beam oscillation and a low welding speed the number of hot cracks can be reduced due to a high curvature at the melt pool end.

Future research activities should focus on the thermo mechanical conditions that lead to transverse hot cracks. For this purpose numerical analysis methods like finite element method (FEM) offer a wide range of possibilities. The aim is to create a hot cracking model which considers both, the metallurgical and the thermo mechanical aspects. Low frequent beam oscillation is a promising way to reduce hot cracks. The results presented in this paper are just a short outlook to the possibilities given by beam oscillation. Beyond that only few data is available concerning the effect of micro defects to the loading capacity of weld seams.

References

Heidrich, W., 2010. Aluminium – ein Leichtbauwerkstoff – viele Anwendungsmöglichkeiten. DVS-Berichte Band 266, Strahlschweißen von Aluminium. DVS Media. Düsseldorf, p. 7.

Zaeh, M., F., Moesl, J., Musiol, J., Oefele, F., 2010. Material Processing with Remote Technology – Revolution or Evolution. LANE 2010. Physics Procedia 5, p. 19.

Schuster, J., 2004. Heißrisse in Schweißverbindungen. Habilitation TU Chemnitz. DVS- Berichte Band 233, Düsseldorf

Katgerman, L., Eskin, D., G., 2008. In Search of the Prediction of Hot Cracking in Aluminium Alloys, in "*Hot Cracking Phenomena in Welds II*" Böllinghaus, T., Herold, H., Cross, C., E., Lippold, C., J., (Eds.). Springer-Verlag. Berlin Heidelberg, p. 3.

Dilthey, U., 2005. Schweißtechnische Fertigungsverfahren 2, Verhalten der Werkstoffe beim Schweißen. 3., bearbeitete Auflage. Springer-Verlag. Berlin Heidelberg.

Schinzel, C., M., 2002. Nd:YAG-Laserstrahlschweißen von Aluminiumwerkstoffen für Anwendungen im Automobilbau. Dissertation Universität Stuttgart. Herbert Utz Verlag. München.

Coniglio, N., Cross, C., E., Michael, T., Lammers, M., 2008. Defining a Critical Weld Dilution to Avoid Solidification Cracking in Aluminium. Welding Journal Vol. 87, p. 237.

Weller, D., Bezençon, C., Stritt, P., Weber, R., Graf, T., 2013. Remote laser welding of multi-alloy aluminium at close edge position. Lasers in Manufacturing Conference 2013. Physics Procedia 41, p. 164.

Rapp, J., 1996. Laserschweißeignung von Aluminiumwerkstoffen für Anwendungen im Leichtbau. Dissertation Universität Stuttgart. B. G. Teubner. Stuttgart.

Thang, Z., 2014. Heißrissvermeidung beim Schweißen von Aluminiumlegierungen mit einem Scheibenlaser. Dissertation Universität Bremen. BIAS Verlag. Bremen.

Hilbinger, R., M., 2000. Heißrissbildung beim Schweißen von Aluminium in Blechrandlage. Dissertation Universität Bayreuth. Herbert Utz Verlag. München.

Ploshikhin, V., Prikhodovsky, A., Makhutin, M., Ilin, A., Zoch, H., W., 2005. Integrated Mechanical-Metallurgical Approach to Modeling of Solidification Cracking in Welds, in "*Hot Cracking Phenomena in Welds*" T. Böllinghaus, H. Herold, (Eds). Springer-Verlag. Berlin Heidelberg, p. 223.

Stritt, P., Weber, R., Graf, T., Mueller, S., Weberpals, J., P., 2012. New hot cracking criterion for laser welding in close-edge position. 31st International congress on applications of lasers & electro-optics. Anaheim, USA, paper #1003.

Oefele, F., Roos, C., 2014. Remote Laser beam welding with inline seam tracking. EALA – European Automotive Laser Application 2014, Bad Nauheim, Germany.

Bachhofer, A., 2000. Schneiden und Schweißen von Aluminiumwerkstoffen mit Festkörperlasern für den Karosseriebau. Dissertation Universität Stuttgart. Herbert Utz Verlag. München.

Waldmann, H., 2001. Werkstofftechnische Aspekte des Laserstrahlschweißens von Alumiumlegierungen für den Fahrzeugbau. Dissertation Universität Bayreuth. Herbert Utz Verlag. München.

DIN EN ISO 6520-1: Schweißen und verwandte Prozesse – Einteilung von geometrischen Unregelmäßigkeiten an metallischen Werkstoffen – Teil 1: Schmelzschweißen. Beuth Verlag. Berlin.

Pellini, W., S., 1952. Strain Theory of Hot Tearing. Foundry issue 80 November, p. 124.

Ehrhardt, A., 1999. Steigerung der Prozeßsicherheit beim Laserstrahlschweißen von Aluminiumlegierungen. Dissertation RWTH Aachen. Shaker Verlag. Aachen.

Hu, B., Richardson, I, M., 2006. Mechanism and possible solution for transverse solidification cracking in laser welding of high strength aluminium alloys. Materials Science and Engineering A 429, p. 287.

Ploshikhin, V., Prikhodovsky, A., Zoch, H., W., 2004. Technologische Maßnahmen zur Vermeidung der Heißrissbildung beim Schweißen von Aluminiumlegierungen. DVS-Berichte Band 229, Schweißen und Löten im Luft- und Raumfahrzeugbau. DVS Media. Düsseldorf, p. 46.

David, S., A., Vitek, J., M., 1989. Correlation between solidification parameters and weld microstructures. International Materials Reviews 1989, Vol. 34, No. 5, p. 213.

Zhang, J., Weckman, D., C., Zhou, Y., 2008. Effects of Temporal Pulse Shaping on Cracking Susceptibility of 6061-T6 Aluminium Nd:YAG Laser Welds. Welding Journal Vol. 87, p. 18.